Regular Article

Dynamics of active run and tumble and passive particles in binary mixture

Vivek Semwal[2,a], Anish Kumar[1,b], Jay Prakash Singh[3,c], and Shradha Mishra[1,d]

[1] Indian Institute of Technology (BHU) Varanasi, Varanasi 221005, India
[2] RIKEN Center for Biosystems Dynamics Research, Kobe, Japan
[3] Israel Institute of Technology Technion, 3200003 Haifa, Israel

Abstract We study a binary mixture of disk-shaped active run and tumble particles (RTPs) and passive particles on a two-dimensional substrate. Both types of particles are athermal. The particles interact through the soft repulsive potential. The activity of RTPs is controlled by tuning their tumbling rate. The system is studied for various sizes of passive particles keeping size of RTPs fixed. Hence the variables are, size ratio (S) of passive particles and RTPs, and the activity of RTPs, v. The characteristic dynamics of both RTPs and passive particles show a crossover from early-time superdiffusive to later-time diffusive. Furthermore, we observed that passive particles dynamics changes from diffusive to subdiffusive with respect to their size. Moreover, late time effective diffusivity D_{eff} of passive particles decreases with increasing their size as in the corresponding equilibrium Stokes systems. We calculated the effective temperatures, using D_{eff}, $T_{a,eff}(\Delta)$ and also using speed distribution $T_{a,eff}(v)$ and compared them. The both $T_{a,eff}(\Delta)$ and $T_{a,eff}(v)$ increases linearly with activity and are in agreement with each other. Hence we can say that an effective equilibrium can be established in such a binary mixture. Our study can be useful to study the various biological systems like; dynamics of passive organelles in cytoplasm, colloids etc.

1 Introduction

In the recent years, researchers have paid lots of attention in the field of active matter [1–6] because of their unusual properties in comparison to their equilibrium counterparts. Examples of active systems range from microscale such as bacterial colonies, cell suspension, artificially designed microparticles [7–12], etc. to the larger scale; fish school, flock of birds [13–15] etc. Active system continuously evolve with time which leads to non-equilibrium class with interesting features i.e; pattern formation [16], non-equilibrium phase transition [17–20], large density fluctuations [21], enhanced dynamics [9, 22, 23], motility-induced phase separation [24–27] etc. In recent years, the motion of passive particles in the presence of an active medium is used to explore the non-equilibrium properties of the medium. In such mixtures passive particles exhibit enhanced diffusivity D_{eff} greater than their thermal (Brownian) diffusivity D_0 [28, 29]. In the experiment of [30], passive Brownian disks in active bacterial solution show enhanced diffusivity. The enhanced diffusivity D_{eff} increases linearly with increasing concentration of bacteria in the solution [31–33]. A variety of studies have focused on the role of bacterial concentration on passive particles [7, 34–36]. In the absence of bacteria, or in equilibrium fluid the diffusivity of a sphere follows the Stokes-Einstein relation [37]. To understand the role of particle size on their dynamics in the active medium, we introduce a binary mixture of RTPs and passive particles. RTPs move in a straight line for some time and then undergo a random rotation (tumble event).

Hence activity can also be tuned with tumbling rate. A large tumbling rate means a smaller run time and hence more random motion.

[a] e-mail: viveksemwal.rs.phy17@itbhu.ac.in

[b] e-mail: anishkumar.rs.phy22@itbhu.ac.in

[c] e-mail: jayps.rs.phy16@itbhu.ac.in

[d] e-mail: smishra.phy@itbhu.ac.in (corresponding author)

We studied the mixture for different sizes of passive particles and the activity of RTPs. Effective diffusivity D_{eff} of RTPs does not change significantly whereas it decreases linearly with size for the passive particles: similar to their equilibrium counterparts-Stokes system [37]. We calculated the effective temperatures, using D_{eff}, $T_{a,eff}(\Delta)$ and using speed distribution of RTPs, $T_{a,eff}(v)$.

The both increase linearly with increasing activity for all size ratios. Hence although the system is active, an effective equilibrium can be established in such mixtures.

The rest of paper is organised as follows. In section 2 we discuss the model with simulation details. In section.3 we discuss the results followed by the conclusion in section 4 at the end.

2 Model

We consider a binary mixture of N_a small RTPs of radius r_a, and N_p passive particles of radius r_p moving on a two-dimensional (2D) substrate of size $L \times L$. The size of the RTPs is kept fixed whereas the size of passive particles is tuned. We define the size ratio $S = r_p/r_a$. The position vector of the centre of the ith RTP and passive particle at time t is given by $\mathbf{r}_i^a(t)$ and $\mathbf{r}_i^p(t)$, respectively. The orientation of ith RTP is represented by a unit vector $\mathbf{n}_i = (\cos\theta_i, \sin\theta_i)$. The dynamics of the RTPs is governed by the overdamped Langevin equation [38–40]

$$\partial_t \mathbf{r}_i^a = v_0 \mathbf{n_i} + \mu_1 \sum_{j \neq i} \mathbf{F}_{ij} \tag{1}$$

The first term on the right-hand side (RHS) of Eq. 1 is due to the activity of the RTPs, and v_0 is the self-propulsion speed. In the second term, μ_1 is the mobility of RTPs and F_{ij} is the soft repulsive interaction (force) among the particles. It is obtained from the binary soft repulsive pair potential $V(r_{ij}) = \frac{k(r_{ij}-2\sigma)^2}{2}$ and $\mathbf{F}_{ij} = -\nabla V(r_{ij})$, for $r_{ij} \leq \sigma$ and zero otherwise. $\sigma = a_i + a_j$, where $a_{i,j}$ is the radius of ith and j^{th} particles respectively. $r_{ij} = |r_j - r_i|$ is the distance between particles i and j. The summation runs over all the particles. $\tau = (\mu k)^{-1}$ sets the elastic time scale in the system. Further, the orientation of RTPs is controlled by run and tumble events. The particles orientation is updated by Eq. 2 introducing a uniform random number r_n. A tumbling rate λ is defined such that if $\lambda > r_n$ then the particle undergoes a tumble event with a random orientation $\eta_i \in (-\pi, +\pi)$. Else it undergoes run event with the same angle as in the previous step. Hence large tumbling rate λ means frequent change in particle orientation. Hence, the orientation update of RTPs is given by:

$$\theta_i(t + \Delta t) = \theta_i(t) + \eta_i(t) \tag{2}$$

The position of the passive particles is also governed by the overdamped Langevin equation,

$$\partial_t \mathbf{r}_i^p = \mu_2 \sum_{i \neq j} \mathbf{F}_{ij} \tag{3}$$

The $\mathbf{F}_{ij}$ has the same form as defined in Eq. 1 and μ_2 is the mobility of passive particles. For the simplicity we kept $\mu_1 = \mu_2$ There is no translational noise [41] in Eqs. 1 and 3, therefore, both RTPs and passive particles are athermal in nature. The smallest time step considered is $\Delta t = 5 \times 10^{-4}$, much smaller than the elastic time scale $\tau = 1$ (for $\mu = 1$ and $k = 1$) All the physical quantities calculated here are averaged over 50 independent realizations. The self-propulsion speed v_0 is kept fixed to 0.5 and activity is varied by tuning tumbling rate λ, such that the dimensionless activity defined as $v = v_0/\lambda r_a$ can vary from 5×10^3 to 5×10^4. We start with random initial positions with non-overlapping condition for all the particles (RTPs and passive particles) and random orientation directions of all RTPs. Once the update of the above two equations is done for all $N = N_a + N_p$ particles, it is counted as one simulation step. We simulated the system for a total of 2×10^5 steps. Total packing fraction of RTPs and passive particles is fixed $\frac{\pi(N_a r_a^2 + N_p r_p^2)}{L^2} = 0.6$. We choose the total area fraction or packing fraction of particles fixed to 0.6 because for very low packing fraction we might not see the interesting effect of RTPs as observed in the previous study on active Borwnian particles (ABPs) [34]. For packing fraction larger than 0.6, particles may not have sufficient space for their dynamics. Also, for the collection of disks in two-dimensions, 0.6 is the random close packing density [42]. The linear dimensions of the system is fixed to $L = 150 r_a$. We have kept the packing fraction of active and passive particles fixed to 0.5 and 0.1 respectively. Since the size of active particle is fixed for different parameters. Hence if the box size is fixed the number of active particles is fixed and number of passive particles will change for different size ratio. Number of active particles in our current simulation is about 4000.

3 Results

3.1 Dynamics of the particles in the mixture

We characterise the dynamics of both types of particles in the mixture for different system parameters (size ratio S and activity v). We first calculate the displacement of RTPs, and passive particles and calculate their mean-square displacement (MSD); $\Delta_{a,p}(t) = \langle |\mathbf{r}(t+t_0) - \mathbf{r}(t_0)|^2 \rangle$. The subscripts a and p denote the active and passive particles respectively. $< .. >$, implies average over different reference times t_0's, for all the particles of respective types and over 50 independent realizations.

The Fig. 2(a, b) shows the plot of MSD of RTPs, $\Delta_a(t)$ for different size ratio S=2, 4, 6, and 8 for two activities $v = 5 \times 10^4$ and $v = 1.2 \times 10^4$ respectively. We find that $\Delta_a(t)$ is independent of the size ratio S for both activities and shows an early-time superdiffusion to late time diffusive dynamics. In general, the particle follows the persistent random walk (PRW) and MSD can be approximated as [43]-

$$\Delta(t) = 2dD_{eff}t[1 - \exp(\frac{-t}{t_c})] \tag{4}$$

where D_{eff} is the effective diffusivity in the steady state and t_c is the typical crossover time from superdiffusive to diffusion. The effective diffusivity of RTPs, $D_{a,eff}$ shows weak dependence with size as shown in Fig. 3(a). Starting from a very small size ratio, effective diffusivity increases with size ratio and then reaches a maximum around $S = 4$ and then again decreases for a large size ratio. For every large size ratios $S > 7$ data further shows the variation with size ratio.

In Fig. 2(c, d) we show the plot of MSD of passive particles $\Delta_p(t)$ for different size ratios. The dashed and solid lines are lines with slope 2 and 1 respectively. For small size ratio, the MSD is diffusive at the late time and becomes subdiffusive for large S as shown by the dotted-dashed line in Fig. 3(c, d). Since for large size ratio $S > 4$, the late time dynamic of passive particles is subdiffusive, the typical crossover time from initial superdiffusive to late time diffusive for ($S \le 4$) and subdiffusive for ($S > 4$) is the time where MSD starts to deviate from t^2. The crossover time $t_{p,c}$ increases linearly with S for both activities as shown in Fig. 3(c) Hence larger passive particles spend more time in superdiffusive propagation. The bigger passive particle are surrounded by more number of RTPs, and resultant persistent motion of RTPs are leading to the increase in crossover time $t_{p,c}$. We further calculated the dependence of effective diffusivity of passive particles, $D_{p,eff}$ on size ratio S. The $D_{p,eff}$ decreases inversely as a function of size ratio as shown in Fig. 3(b). It matches with the earlier results for the diffusion of Brownian disk moving in the equilibrium Stokes fluid [37].
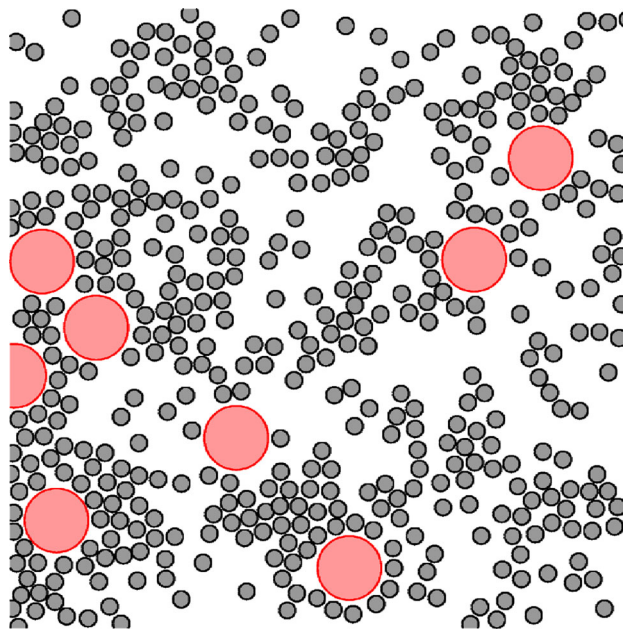

Fig. 1 (color online) Typical snapshot (from the simulation) of the part of the system of binary mixture. RTPs (black particles) and passive particles (red particles). The two parameters $S = 4$ and $v = 5 \times 10^4$

We also explored the system for fixed size ratios $S = 1$ and $S = 8$ and varying the activity v. For all activities, the RTPs show PRW as given in Eq. 4 and MSD shows a crossover from early-time superdiffusive to late-time diffusive behaviour. In Fig. 4(a, b) we show the plot of MSD of RTPs particles, $\Delta_a(t)$ for different v and fixed size ratios $S = 1$ and 8 respectively. The data points from the numerical simulation and lines are fit from the expression of MSD as given in Eq. 4. Fitting line is only drawn for $v = 5 \times 10^4$ as shown by solid line in Fig. 4(a, b). The $t_{a,c}$ is obtained by fitting the MSD $\Delta_a(t)$ of RTPs with the expression of PRW as given in Eq. 4. In Fig. 5 we plot the crossover $t_{a,c}$ vs. v. The $t_{a,c}$ increases linearly with increasing v as shown in Fig. 5. We also calculated the $D_{a,eff}$, obtained from the fitting. The variation of $D_{a,eff}$ with activity will be discussed later.

To further confirm that the MSD follows the PRW, we show the scaling collapse of MSD by rescaling the $x-$axis with $t_{a,c}$ (scaled time $t/t_{a,c}$) and $y-$axis, as rescaled MSD, $\frac{\Delta_a(t)}{D_{a,eff}t_{a,c}}$. We find scaling collapse of data for both size ratios and for all activities as shown in the inset of Fig. 4(a, b).

We also calculated the MSD of passive particles $\Delta_p(t)$ for different activities and for the two size ratios $S = 1$ and $S = 8$ as shown in Fig. 4(c-d).Label For small size ratio $S = 1$, the passive particles also show a crossover
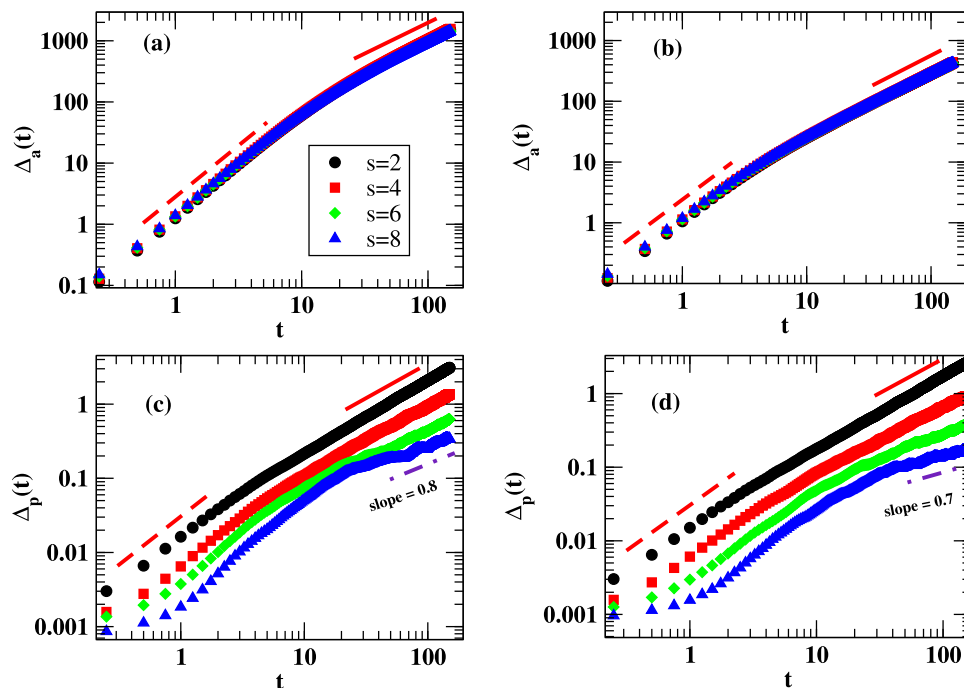

Fig. 2 (color online) Plot $\Delta_a(t)$ vs. t for active (**a, b**) and passive particles $\Delta_p(t)$ (**c, d**), for activity $v = 5 \times 10^4$, 1.2×10^4 with variation of different size ratios S. Dashed and solid lines are lines with slope 2 and 1 respectively. The dotted dashed line in (**c**) and **d** is of slope 0.8 and 0.7 respectively
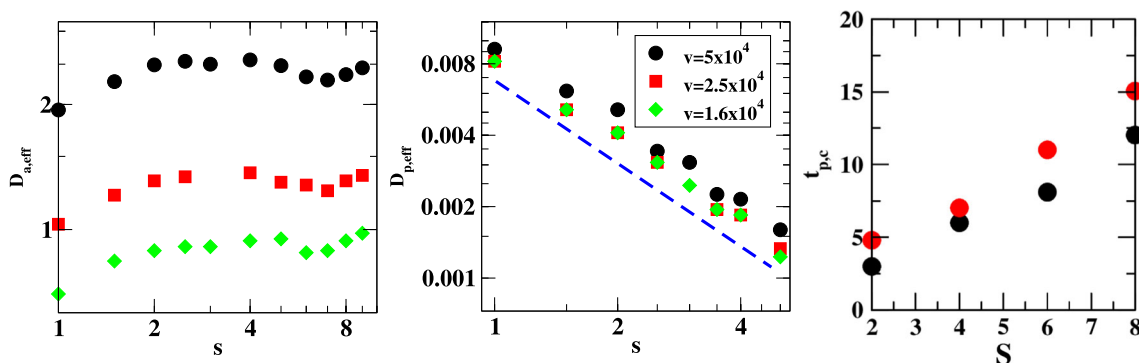

Fig. 3 (color online) Plot shows variation of $D_{a,eff}$ with size ratio S for different activity v for active particles. **a** $D_{p,eff}$ vs. S for passive particles. The dashed line has a slope -1. **b** $t_{p,c}$ for passive particles with size ratios S for two different $v = 5 \times 10^4$ (black circles) and 1.6×10^4 (red circles). **c** (Error bars are of the order of symbol size)
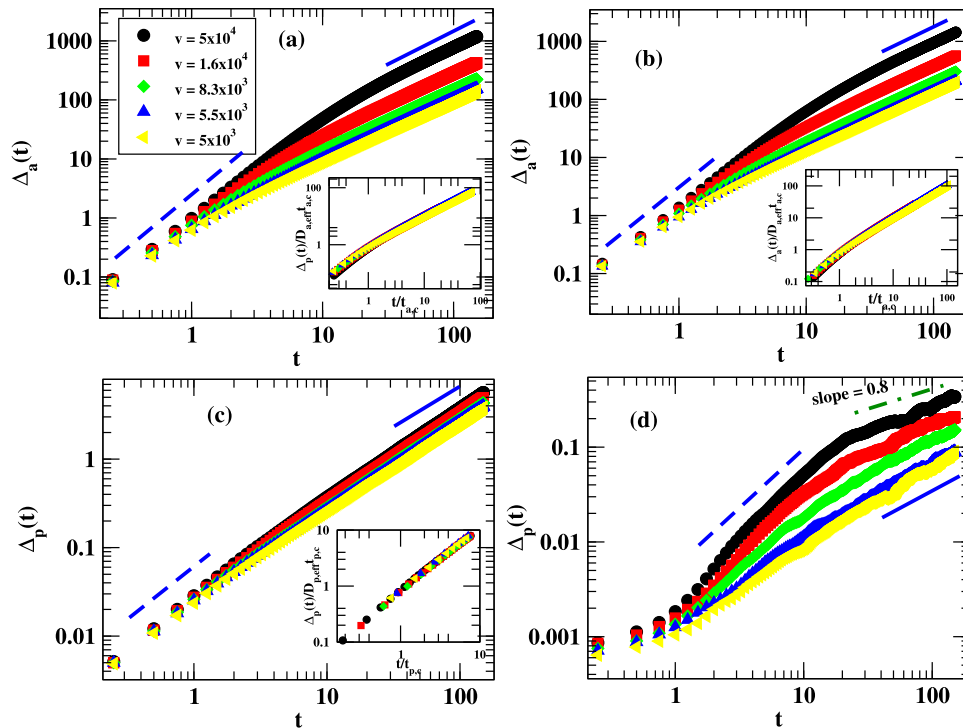
Fig. 4 (color online) The Plots (**a–d**) show the $\Delta(t)$ vs. t for active $\Delta_a(t)$ (**a, b**) and $\Delta_p(t)$ passive particles (**c, d**) for $S = 1$ and 8 respectively. with different v (inset shows the scaling plot of MSD). lines are fitting function using Eqn. 4. solid and dashed lines in (**a–c**) are of slope 2 and 1 respectively. The dotted dashed lines in (**d**) is of slope 0.8
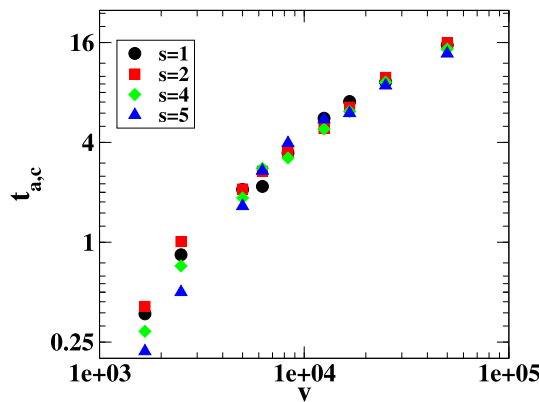

Fig. 5 (color online) **a** Plot of variation of $t_{a,c}$ with v for different size ratios S

from early time superdiffusive to late time diffusive behavior and MSD $\Delta_p(t)$ fits well with the expression for the PRW as given in Eq. 4. Data shows a scaling collapse when we plot the scaled time $t/t_{p,c}$ vs. scaled MSD, $\frac{\Delta_p(t)}{D_{p,eff}t_{p,c}}$ 4(c) (inset). For a large size ratio, $S = 8$, passive particles show an early-time superdiffusion but late time subdiffusion with $\Delta_p(t) \simeq t^{0.8}$, as shown by the dotted dashed in Fig. 4(d). The early-time superdiffusion to late time subdiffusion appears for larger activities $v \geq 8.3 \times 10^3$. But for small activities $v < 8.3 \times 10^3$, it is diffusive for the whole range of time as shown by the solid line in Fig. 4(d)

We also investigated the dynamic of particles by extracting the MSD dynamic exponent $\beta(t)$ defined by $\Delta(t) \sim t^{\beta(t)}$, hence

$$\beta(t) = log_{10}\left[\frac{\Delta(10t)}{\Delta(t)}\right] \tag{5}$$

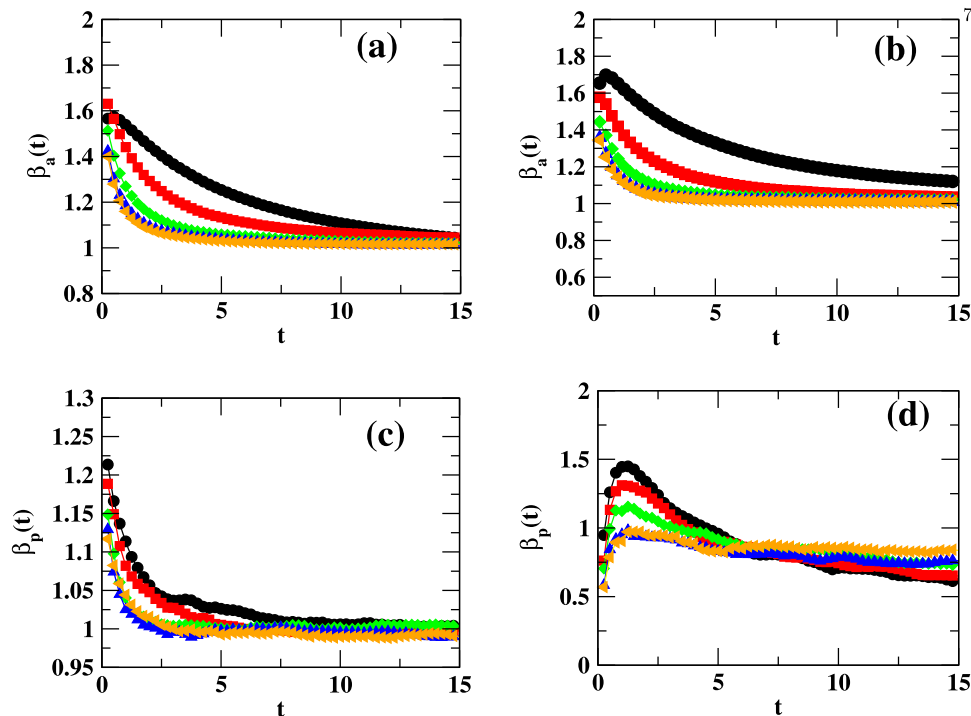**Fig. 6** (color online) In these plot we shows the $\beta(t)$ vs t, for active $\beta_a(t)$ (**a, b**) and passive $\beta_p(t)$ (**c, d**). Other parameters are the same as in Fig. 4

The Fig.6(a-d) shows the plot of dynamic exponent $\beta(t)$ vs. time t for the same parameter as in 4(a-d) respectively. For the RTPs $\beta_{(a)}(t)$ shows crossover from superdiffusive $\beta_a(t) > 1$ to diffusive $\beta_a(t) \sim 1$ regime. For the passive particles for $S = 1$, early time dynamics is superdiffusive $\beta_p(t) > 1$ and becomes diffusive $\beta_p \sim 1$ at late times. Whereas for the size ratio 8 passive particles show superdiffusion $\beta_p(t) > 1$ to subdiffusive $\beta_p < 1$ motion at late times. The dynamic exponent approaches to 1 for late times on decreasing activity v.

3.2 Diffusivity and effective temperature of active particles in the mixture

Now we further explore the concept of effective temperature [43–46] of the medium. Assuming an effective equilibrium, a relation between an effective temperature (calculated from the speed distribution) $T_{a,eff}(v)$ and effective diffusivity calculated from MSD of active particles can be obtained. The effective temperature calculated from MSD is defined as $T_{a,eff}(\Delta) = D_{a,eff}/k_B$, where k_B is a constant factor used as the fitting parameters.

To calculate $T_{a,eff}(v)$, we first calculate the speed distribution $p(\sigma)$ of RTPs. The fluctuation in the speed distribution is the measure of the randomness present in the system. If the distribution follows a Maxwell-Boltzmann (MB) form as always the case in fluids at equilibrium, the mean kinetic energy is related to the thermodynamic temperature via the equipartition theorem [43]. We calculate the $p(\sigma)$ and it follows the MB distribution for different parameters. fitted it with standard MB distribution. In Fig. 7(a) we plot $p(\sigma)$ for different size ratio S. The data points are from the numerical simulation and lines are fit to MB distribution. Further, we compared the two effective temperatures of active particles, calculated from speed distribution $p(\sigma)$; $T_{a,eff}(v)$ and from the MSD $T_{a,eff}(\Delta)$.

In Fig. 7(b) we plot the variation of $T_{a,eff}(v)$ and $T_{a,eff}(\Delta)$ vs. v for different S. The data shows good match of both the effective temperatures. In RTP system [47] $D_{eff} = v_0^2/d\lambda = v_0 v r_a/d$. Where d is the dimensionality of space. Hence $T_{a,eff}(\Delta)$ varies linearly with v as shown in Fig. 7(b). For better comparison, we also tabulated the data for the two effective temperatures in table 1 for four different size ratios and varying activity.

4 Summary

We extensively studied the dynamics in a binary mixture of disk-shaped active RTPs and passive particles on a two-dimensional substrate. Both types of particles are athermal in nature. The activity of RTPs is controlled by
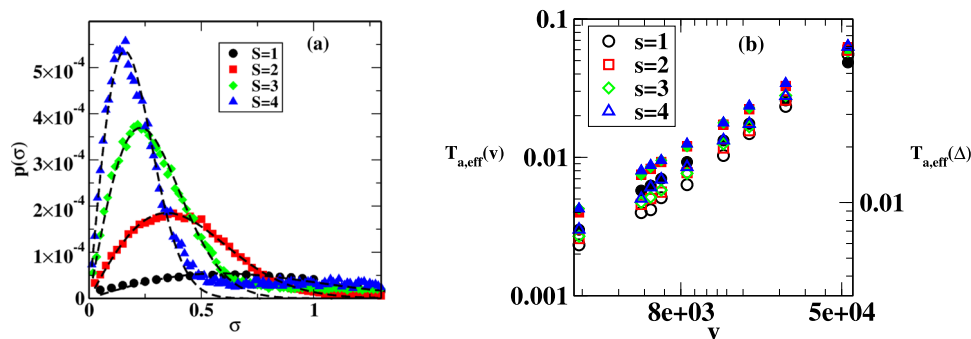
Fig. 7 (color online) **a** speed distribution and **b** $T_{a,eff}(\Delta)$ (open symbol) and $T_{a,eff}(v)$ (solid symbol) vs. v for different size ratio

Table 1 Table shows the variation of the effective temperature calculated from MSD and speed distribution as a function of activity and four different size ratios. All the data with the error of order $\pm\ 0.001$

v	S = 1		S = 2		S = 3		S = 4	
	$T_{a,eff}(v)$	$T_{a,eff}(\Delta)$	$T_{a,eff}(v)$	$T_{a,eff}(\Delta)$	$T_{a,eff}(v)$	$T_{a,eff}(\Delta)$	$T_{a,eff}(v)$	$T_{a,eff}(\Delta)$
16666	0.018	0.024	0.022	0.024	0.023	0.026	0.023	0.027
12500	0.013	0.018	0.017	0.020	0.018	0.021	0.018	0.022
8333	0.009	0.012	0.012	0.015	0.012	0.014	0.012	0.016
6250	0.007	0.011	0.009	0.011	0.009	0.012	0.010	0.013
5555	0.006	0.009	0.008	0.010	0.009	0.011	0.009	0.012
5000	0.006	0.009	0.007	0.010	0.008	0.010	0.008	0.011
2500	0.003	0.006	0.004	0.006	0.004	0.006	0.004	0.007

their tumbling rate. The size of RTPs is fixed whereas it is varied for passive particles. Further, in the mixture, the MSD of RTPs show early-time superdiffusive behavior and late-time diffusive motion with increasing value of v and size ratio S. The passive particles show a crossover from late time subdiffusive to diffusive dynamics on increasing v and decreasing S. The late-time effective diffusivity of passive particles $D_{p,eff}$ decay monotonically with their size as found in equilibrium passive Stokes fluid [37].

The effective diffusivity of RTPs increases linearly with their activity and shows a good match with the effective temperature obtained from the steady-state speed distribution with the MB distribution.

Hence our study explores dynamics and steady-state of RTPs and passive particles in the mixture and shows an effective equilibrium in the system. The particle-size dependence of MSD of passive particles in the presence of active RTPs has important applications in particle sorting in different types of fluids like-microfluidic devices [48].

Data availability statement The data that support the findings of this study are available upon reasonable request from the authors.

References

1. J. Toner, Y. Tu, S. Ramaswamy, Annal. Phys. **318**, 170 (2005)
2. T. Vicsek, A. Zafeiris, Phys. Rep. **517**, 71 (2012)
3. M.C. Marchetti, J.-F. Joanny, S. Ramaswamy, T.B. Liverpool, J. Prost, M. Rao, R.A. Simha, Rev. Mod. Phys. **85**, 1143 (2013)

4. M.E. Cates, J. Tailleur, Annu. Rev. Condens. Matter Phys. **6**, 219 (2015)
5. M.E. Cates, J. Tailleur, Europhys. Lett. **101**, 20010 (2013)
6. S. Ramaswamy, Annu. Rev. Condens. Matter Phys. **1**, 323 (2010)
7. A.E. Patteson, A. Gopinath, P.K. Purohit, P.E. Arratia, Soft Matter **12**, 2365 (2016)
8. U. Choudhury, A.V. Straube, P. Fischer, J.G. Gibbs, F. Höfling, New J. Phys. **19**, 125010 (2017)
9. V. Semwal, S. Dikshit, S. Mishra, Eur. Phys. J. E **44**, 1 (2021)
10. J.R. Howse, R.A. Jones, A.J. Ryan, T. Gough, R. Vafabakhsh, R. Golestanian, Phys. Rev. Lett. **99**, 048102 (2007)
11. H.-R. Jiang, N. Yoshinaga, M. Sano, Phys. Rev. Lett. **105**, 268302 (2010)
12. J. Zhang, B.A. Grzybowski, S. Granick, Langmuir **33**, 6964 (2017)
13. A. Cavagna, I. Giardina, Annu. Rev. Condens. Matter Phys. **5**, 183 (2014)
14. N. Kumar, H. Soni, S. Ramaswamy, A. Sood, Nat. Commun. **5**, 4688 (2014)
15. J.A. Giannini, J.G. Puckett, Phys. Rev. E **101**, 062605 (2020)
16. J. Denk, E. Frey, Proc. Natl. Acad. Sci. **117**, 31623 (2020)
17. K. Gowrishankar, M. Rao, Soft Matter **12**, 2040 (2016)
18. B. Bhattacherjee, S. Mishra, S. Manna, Phys. Rev. E **92**, 062134 (2015)
19. J.P. Singh, S. Kumar, S. Mishra, J. Stat. Mech: Theory Exp. **2021**, 083217 (2021)
20. S. Pattanayak, S. Mishra, J. Phys. Commun. **2**, 045007 (2018)
21. R. Mandal, P.J. Bhuyan, P. Chaudhuri, C. Dasgupta, M. Rao, Nat. Commun. **11**, 2581 (2020)
22. M.R. Shaebani, A. Wysocki, R.G. Winkler, G. Gompper, H. Rieger, Nat. Rev. Phys. **2**, 181 (2020)
23. S. Kumar, J.P. Singh, D. Giri, S. Mishra, Phys. Rev. E **104**, 024601 (2021)
24. G. Gonnella, D. Marenduzzo, A. Suma, A. Tiribocchi, C R Phys. **16**, 316 (2015)
25. F. Kümmel, B. Ten Hagen, R. Wittkowski, I. Buttinoni, R. Eichhorn, G. Volpe, H. Löwen, C. Bechinger, Phys. Rev. Lett. **110**, 198302 (2013)
26. A.P. Solon, Y. Fily, A. Baskaran, M.E. Cates, Y. Kafri, M. Kardar, J. Tailleur, Nat. Phys. **11**, 673 (2015)
27. C. Bechinger, R. Di Leonardo, H. Löwen, C. Reichhardt, G. Volpe, G. Volpe, Rev. Mod. Phys. **88**, 045006 (2016)
28. G. Mino, T.E. Mallouk, T. Darnige, M. Hoyos, J. Dauchet, J. Dunstan, R. Soto, Y. Wang, A. Rousselet, E. Clement, Phys. Rev. Lett. **106**, 048102 (2011)
29. H. Kurtuldu, J.S. Guasto, K.A. Johnson, J.P. Gollub, Proc. Natl. Acad. Sci. **108**, 10391 (2011)
30. X.-L. Wu, A. Libchaber, Phys. Rev. Lett. **84**, 3017 (2000)
31. M.J. Kim, K.S. Breuer, Phys. Fluids **16**, L78 (2004)
32. K.C. Leptos, J.S. Guasto, J.P. Gollub, A.I. Pesci, R.E. Goldstein, Phys. Rev. Lett. **103**, 198103 (2009)
33. A. Jepson, V.A. Martinez, J. Schwarz-Linek, A. Morozov, W.C. Poon, Phys. Rev. E **88**, 041002 (2013)
34. P. Dolai, A. Simha, S. Mishra, Soft Matter **14**, 6137 (2018)
35. S. Gokhale, J. Li, A. Solon, J. Gore, N. Fakhri, Phys. Rev. E **105**, 054605 (2022)
36. P. Kushwaha, V. Semwal, S. Maity, S. Mishra, V. Chikkadi, Phys. Rev. E **108**, 034603 (2023)
37. A. Einstein et al., Ann. Phys. **17**, 208 (1905)
38. Y. Fily, M.C. Marchetti, Phys. Rev. Lett. **108**, 235702 (2012)
39. S. Ramaswamy, J. Stat. Mech: Theory Exp. **2017**, 054002 (2017)
40. É. Fodor, M.C. Marchetti, Phys. A **504**, 106 (2018)
41. G.E. Uhlenbeck, L.S. Ornstein, Phys. Rev. **36**, 823 (1930)
42. A. Magazinov, Commun. Math. Phys. **364**, 1 (2018)
43. P. D. Beale, *Statistical Mechanics* (Butterworth-Heinemann, 1996)
44. D. Loi, S. Mossa, L.F. Cugliandolo, Soft Matter **7**, 3726 (2011)
45. E. Ben-Isaac, Y. Park, G. Popescu, F.L. Brown, N.S. Gov, Y. Shokef, Phys. Rev. Lett. **106**, 238103 (2011)
46. E. Ben-Isaac, É. Fodor, P. Visco, F. Van Wijland, N.S. Gov, Phys. Rev. E **92**, 012716 (2015)
47. J. Tailleur, M. Cates, Phys. Rev. Lett. **100**, 218103 (2008)
48. S.C. Abeylath, E. Turos, Expert Opin. Drug Deliv. **5**, 931 (2008)